Vascular Endothelial Growth Factor Receptor 1 Morpholino Decreases Angiogenesis in a Murine Corneal Suture Model

Yang Kyung Cho,[1,2] *Hironori Uehara,*[1] *Jason R. Young,*[1] *Bonnie Archer,*[1] *Xiaohui Zhang,*[1] *and Balamurali K. Ambati*[1]

Purpose. This study sought to determine whether a vascular endothelial growth factor receptor 1 (VEGFR1)–specific morpholino could induce the alternative splicing of Flt-1 pre-mRNA to downregulate membrane-bound Flt-1 (mFlt-1) and increase the production of soluble Flt-1 (sFlt-1), thereby limiting angiogenesis and inflammation in a mouse corneal suture injury model.

Methods. A murine corneal suture model was used to investigate the effects of a VEGFR1-specific morpholino in vivo. Western blot analysis and RT-PCR were used to compare the impact of the Flt morpholino on mFlt-1 and sFlt-1 levels. For vascular regression modeling, two corneal sutures were placed and injected with Flt morpholino, standard morpholino, and PBS on days 8 and 10. Corneas were harvested on day 14. The grade of neovascularization (graded 0–5; 0, no neovascularization; 5, thick tortuous new vessel growth over the suture and toward the center of the cornea) was compared on days 8, 10, and 14. Immunohistochemistry, fluorescent microscopy, and confocal microscopy were used to digitally quantify the area and volume of neovascularization and inflammatory infiltration.

Results. Western blot analysis revealed that the Flt morpholino decreased mFlt-1 levels while increasing sFlt-1 levels. An increased sFlt-1/mFlt-1 ratio in the Flt morpholino group was seen with RT-PCR. Based on the neovascularization grading, there was a decrease in neovascularization area in the Flt morpholino group (3.29 ± 0.19 to 2.92 ± 0.13) from day 8 to 14 ($P < 0.05$) compared with that in both the standard morpholino (2.68 ± 0.19 to 3.14 ± 0.22) and in the PBS (2.96 ± 0.14 to 3.42 ± 0.19) groups, both of which showed an increase in neovascularization ($P < 0.05$). The Flt morpholino group also showed reduced neovascularization volume compared with that of the PBS ($P = 0.001$) and STD morpholino groups ($P = 0.000$).

Conclusions. Flt morpholinos decrease mFlt-1 and increase sFlt-1 levels, resulting in decreased neovascularization in a murine corneal suture model. (*Invest Ophthalmol Vis Sci.* 2012;53:685–692) DOI:10.1167/iovs.11-8391

Corneal angiogenesis is a pathologic process associated with many diseases and complications involving the anterior eye. Infectious and inflammatory conditions associated with corneal angiogenesis include herpes keratitis, *Pseudomonas*, pemphigoid, and atopic conjunctivitis. Neurotrophic ulcer, ischemia due to limbal stem cell deficiency, and trauma including extended contact lens wear and alkali burns can also contribute to this pathologic process.[1] Corneal angiogenesis is also a recognized risk factor for immunologic rejection[2] and is one of the most important causes of corneal graft failure[3] in penetrating keratoplasty (PK). This process contributes to rejection rates in high-risk PK patients of >70%,[4] with up to 28% of grafts requiring repeat transplantation.[5] As a result, therapies aimed at reducing corneal angiogenesis have the potential to improve the outcomes of patients with corneal disease.

Corneal angiogenesis is driven by vascular endothelial growth factor-A (VEGF-A) and plays an important pathogenic role in a variety of ocular surface diseases.[6,7] VEGF acts by binding tyrosine kinase receptors on the cell surface, causing them to dimerize and become activated through phosphorylation.[6,8] Angiogenic responses to VEGF-A are mediated by vascular endothelial growth factor receptor 1 (VEGFR-1, Flt-1) and VEGFR-2 (KDR). Although the tyrosine kinase activity of VEGFR-1 is usually weaker than that of VEGFR-2, VEGFR-1 has stronger VEGF-binding affinity than that of VEGFR-2.[7,9] Furthermore, VEGFR-1 is involved in the VEGF-dependent migration and gene expression of monocytes and macrophages.[9–11] VEGFR-1 has two isoforms: a full-length membrane-bound form (mFlt-1) and a shorter soluble (nonmembrane bound) form.[8,9,12]

Soluble VEGFR-1 (sFlt-1) can be derived from alternative splicing of VEGFR-1 or from proteolytic cleavage of the ectodomain from the cell surface.[8,13] The molecular role of sFlt-1 is believed to be the sequestration of the VEGF ligands, resulting in decreased activation of VEGF receptors. Potential biological functions of sFlt-1 have been deduced from its capacity to neutralize VEGF and include inhibiting angiogenesis by dampening the VEGF–VEGFR2 signaling pathway and by acting as an anti-inflammatory through attenuating VEGF–VEGFR1 signaling, thus decreasing monocyte and macrophage activation and migration.[6,8] As a result, the splicing control between mFLT-1 and sFLT1 may lead to suppression of angiogenesis and inflammation.

Morpholinos are synthetic molecules that are similar to DNA oligonucleotides that can bind mRNA to sterically block the molecular machinery of translation or alternative splicing.[14–18] Although morpholinos have been shown to be very effective for splice modification by blocking splicing events,[19] morpholinos can also be used to block translation of mRNA or

From the [1]Department of Ophthalmology, University of Utah School of Medicine, Salt Lake City, Utah; and the [2]Department of Ophthalmology, St. Vincent Hospital, The Catholic University of Korea, Suwon, South Korea.

Supported by National Institutes of Health/National Eye Institute Grant EY017950.

Submitted for publication August 10, 2011; revised October 30, 2011; accepted December 11, 2011.

Disclosure: **Y.K. Cho**, None; **H. Uehara**, None; **J.R. Young**, None; **B. Archer**, None; **X. Zhang**, None; **B.K. Ambati**, None

Corresponding author: Balamurali K. Ambati, Moran Eye Center, University of Utah, 65 Mario Capecchi Drive, Salt Lake City, UT 84132; bala.ambati@utah.edu.

inhibit microRNA activity, depending on where it specifically binds the RNA.[20] This study sought to determine whether a VEGFR-1–specific morpholino that promotes the shift from mFLT to sFLT can inhibit neovascularization and inflammation in a murine corneal suture model.

Materials and Methods

All experiments were performed in accordance with the regulations of ARVO (Association for Research in Vision and Ophthalmology) and were approved by the Institutional Animal Care and Use Committee of the University of Utah.

Morpholino Oligomer Construction

Morpholino constructs were designed to target the exon 13/intron 13 junction of the murine Flt-1 transcript. The Flt morpholino (VEGFR1_MO: 5′-CTT TTT GCC GCA GTG CTC ACC TCTA-3′) and the nonspecific standard (STD) morpholino (5′-CCT CTT ACC TCA GTT ACA ATT TATA-3′) were synthesized by a commercial modifier of gene expression (Gene Tools, Philomath, OR).

Corneal Suture Model

Balb/c mice (JAX Mice and Services; Jackson Laboratory, Bar Harbor, ME) were anesthetized with intramu[b]scular tribromoethanol (Avertin) and 0.5% proparacaine ophthalmic solution for cornea. Two corneal sutures (11-0 nylon) were placed between the corneal center and the limbus at the 12 and 6 o'clock positions. Topical erythromycin ointment (0.5%) was applied immediately after suture placement.

To determine the effect of the morpholino by Western blot analysis and RT-PCR, four treatment groups were studied: an Flt-1–specific morpholino group, a standard morpholino group, a PBS (Dulbecco's phosphate-buffered saline) group, and a group that did not receive suture placement ("normal cornea" group). The corresponding treatment was injected into the corneal stroma on days 7 and 10. Corneas were harvested on day 11.

To develop the angiogenesis regression model, the mice were divided into three treatment groups: the Flt morpholino group, the standard morpholino group, and the PBS group. Two corneal sutures were placed in each mouse cornea as previously described. The treatments were injected into the corneal stroma on days 8 and 10. This allowed 8 days for inflammation and angiogenesis to occur in the sutured corneal tissue before treatment injection. Corneas were harvested on day 14. Photographs were taken 8, 10, and 14 days after suture placement.

Corneal Intrastromal Injection

A nick in the anterior stroma was made using a 30-gauge needle in the midperiphery of the cornea. A 0.5-inch 33-gauge needle with a 45° bevel on a 10-μL gas-tight syringe (Hamilton, Reno, NV) was used to inject 4 μL of the respective treatment (40 ng/μL of Flt morpholino, 40 ng/μL of standard morpholino, and PBS) through the nick into the corneal stroma. One injection was made per cornea lateral to one of the sutures.

Western Blot

On day 11 after suture placement, two corneas were harvested from each treatment group and were placed in radioimmunoprecipitation assay buffer (Sigma-Aldrich, St. Louis, MO). After sonication and centrifugation, the supernatants were transferred to new tubes. Protein concentration was determined using the bicinchoninic acid assay. Under a reducing condition, 10 μg protein was loaded to SDS-PAGE (10%). After transfer to nitrocellulose membrane, the membrane was blocked with 3% bovine serum albumin (BSA) and 0.1% Tween 20 in Tris-buffered saline (TBST). An antibody to the extracellular antibody of VEGFR1 (BAF471; R&D Systems, Inc., Minneapolis, MN) was used at 1 μg/mL in 3% BSA/TBST. An antibody to the intracellular domain of VEGFR1 (ab2350; Abcam Inc., Cambridge, MA) was used at the same concentration. Appropriate secondary antibodies (HRP conjugated) were used. After washing, the bands were illuminated by a Western blot detection kit (ECL-PLUS; Amersham Biosciences, Pittsburgh, PA) and detected by an electronic imaging system (FOTO/Analyst; Fotodyne Inc., Hartland, WI). Glyceraldehyde-3-phosphate dehydrogenase was used as an internal control.

RNA Extraction, Complementary DNA Synthesis, and Quantification with Real-Time PCR

RNA was isolated using RNA isolation kits (Qiagen, Valencia, CA). cDNA was made from total RNA by using reverse transcriptase (RT) and oligo dT primers according to the manufacturer's instruction. Target RNA was amplified by real-time PCR using primers designed against the soluble and membranous form of VEGFR-1 (QuantiTect SYBR Green PCR Kit; Qiagen, Valencia, CA). mRNA of mFlt-1 and sFlt-1 was quantified.

Grading of Corneal Neovascularization

Microscopic images were captured using a surgical microscope (SZX7; Olympus, Tokyo, Japan) and attached camera (U-TVO.5XC-3; Olympus) before suture placement and at days 8, 10, and 14. Corneal neovascularization around each suture site was graded according to area and intensity of vessel growth from 0 to 5: 0 (no neovascularization), 1 (weak and tiny vessels from the limbus), 2 (new vessels growing between the limbus and corneal suture), 3 (new vessel growth to and around the suture), 4 (thick tortuous new vessel growth to and around the suture), and 5 (thick tortuous new vessel growth over the suture and toward the center of the cornea).

Immunohistochemical Staining

Fourteen days after suture placement, the corneas were harvested and trimmed of any remaining limbus and iris. These corneas were dissected, rinsed in PBS for 30 minutes, and fixed in 100% acetone for 20 minutes. After washing in PBST (0.1% Tween 20/PBS), nonspecific binding was blocked with 3% BSA/PBS for 3 nights at 4°C. Overnight incubation with fluorescein isothiocyanate–conjugated monoclonal anti-mouse CD31 antibody (558738; BD Pharmingen) at a concentration of 1:200 and multicolor flow cytometry application (Alexa Fluor 647 rat anti-mouse CD11b antibody, 557686; BD Pharmingen) at 1:100 in 3% BSA/PBS was done at 4°C. This was followed by four washes in PBST at room temperature. Corneas were mounted with an antifading agent (Gelmount; Biomeda, San Francisco, CA).

Digital Quantification of Neovascularization

After immunochemical staining for vascular endothelial cells and flat mounting of the cornea, images were captured with a fluorescent microscope (Carl Zeiss MicroImaging, Inc., Thornwood, NY). The method of neovascular quantification used in this study has been previously described.[21] Briefly, the area of neovascularization was quantified by setting a threshold level of fluorescence above which only vessels were captured and processed using ImageJ software (developed by Wayne Rasband, National Institutes of Health, Bethesda, MD; available at http://rsb.info.nih.gov/ij/index.html). The total corneal area was outlined using the innermost vessel of the limbal arcade as the border. The total area of neovascularization was normalized to the total corneal area.

A confocal microscope was used to quantify the volume of neovascularization and inflammatory infiltration (Olympus FluoView FV1000; Olympus). Horizontal sections (objective magnification ×10) were obtained from the surface of each suture to the deepest focal plane of neovascularized area, to a maximum depth of 5 μm. Twenty-two to 24 slices of two-dimensional horizontal section images were stacked to create a three-dimensional representation of each suture area using the pixel number of CD31 and CD11b stained volume. The scaling factor (μm/pixel) for each x, y, and z dimension was 1.242, 1.242, and 5.

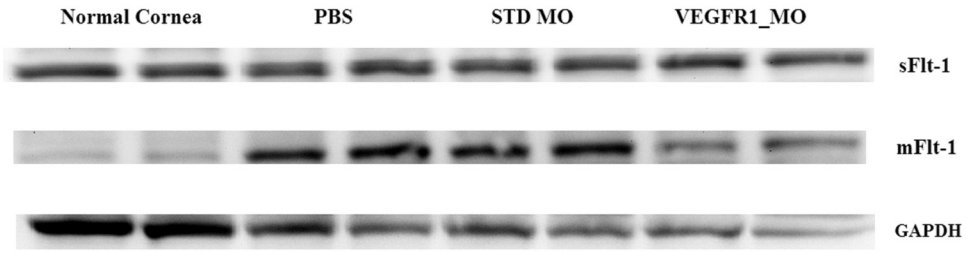

FIGURE 1. Western blot using an antibody specific for the extracellular domain of VEGFR1. An increased band was found around 75 kDa (corresponding to sFlt-1) in the Flt morpholino group. When an antibody specific for the C terminus of VEGFR1 was used, a decreased 80-kDa band (corresponding to mFlt-1) was seen in the Flt morpholino group.

Statistical Analysis

A commercial statistical/analytical software program (SPSS 11.5 for Windows; SPSS, Inc., Chicago, IL) was used for the statistical analysis. A two-tailed paired *t*-test was used to compare the change in biomicroscopic grade in each treatment group. Two-tailed unpaired *t*-tests were used to compare the area and volume of neovascularization and the infiltration of the treatment groups.

RESULTS

Effect of the Morpholino on Flt-1 Expression at the Protein Level

To determine whether the Flt morpholino could promote a shift of mFLT-1 to sFLT-1, we examined sFLT-1 and mFLT-1 protein levels in sutured corneas using Western blot analysis. We used two types of antibody: one that recognized the extracellular domain, which exists in both sFLT-1 and mFLT-1; and the other, which recognized the C-terminal of mFLT-1, which exists only in mFLT-1. Using the antibody recognizing the extracellular domain, an increase in the 75-kDa band was seen (corresponding to sFlt-1) in the Flt morpholino group compared with the other treatment groups (Fig. 1). When an antibody specific for the C terminus of VEGFR1 was used, a decrease in the 80-kDa band was seen in the Flt morpholino group (80-kDa band corresponds to mFlt-1).

Effect of Morpholino on Flt-1 Expression at the mRNA Level

We found a significant difference in the sFlt-1/mFlt-1 ratio between the VEGFR1 morpholino and the STD morpholino treatment groups (Fig. 2, $P = 0.036$), whereas there was no difference between the VEGFR1 morpholino and the PBS treatment groups ($P = 0.449$). The ratio of sFlt-1/mFlt-1 was 1.284 ± 0.122 in the VEGFR1_MO group, 1.154 ± 0.111 in the PBS group, and 1.00 ± 0.050 in the STD MO group.

Comparison of In Vivo Neovascularization by Investigator Grading

There were 24 total suture sites graded in the Flt morpholino group, 28 in the standard morpholino group, and 24 in the PBS

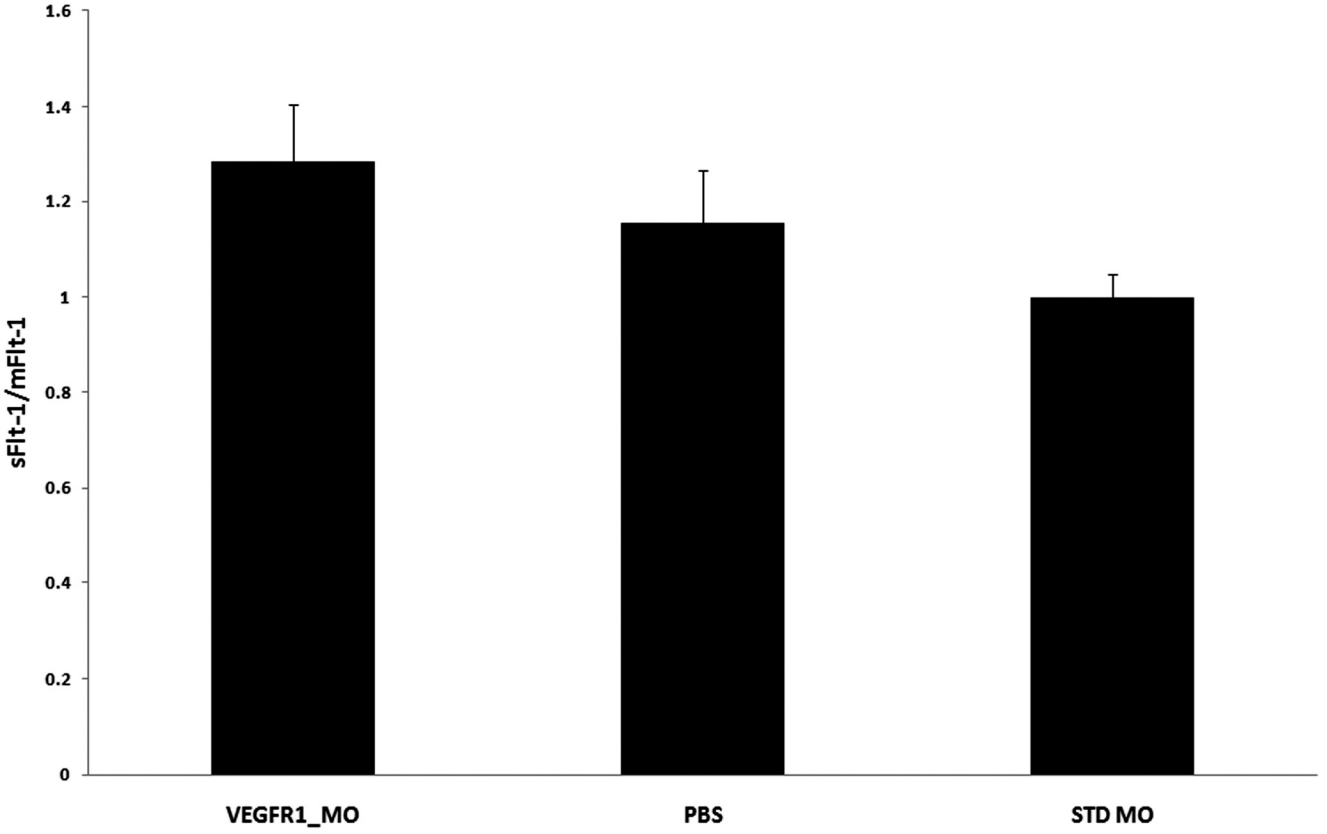

FIGURE 2. RT-PCR. The ratio of sFlt-1/mFlt-1 was increased in the Flt morpholino group compared with the STD morpholino group ($P = 0.035$) and the PBS group ($P = 0.449$).

group (one mouse died in both the Flt morpholino and PBS groups). The comparison between these groups on days 8 and 14 revealed regression of neovascularization in the Flt morpholino group ($P = 0.026$), with an increase of neovascularization in the standard morpholino and PBS groups ($P = 0.001$ and $P = 0.005$; Fig. 3). Specifically, in the Flt morpholino group there was a decrease of neovascularization from day 8 (3.29 ± 0.19) to day 14 (2.92 ± 0.13). In contrast, the standard morpholino group had an increase in neovascularization from 2.68 ± 0.19 (day 8) to 3.14 ± 0.22 (day 14) and the PBS group increased from 2.96 ± 0.14 (day 8) to 3.42 ± 0.19 (day 14).

Comparison of Neovascularization Using Immunostaining and Digital Quantification

To quantify the amount of neovascularization in the mouse cornea, we stained the cornea with CD31 antibody, a marker for vascular endothelial cells. The ratio of the area of neovascularization to the total area of the cornea was 0.185 ± 0.009 in the Flt morpholino group ($n = 12$), 0.227 ± 0.021 in the standard morpholino group ($n = 14$), and 0.231 ± 0.015 in the PBS group ($n = 12$) (Fig. 4). The Flt morpholino group exhibited less neovascularization compared with that of the PBS group ($P = 0.019$), but was not significantly different compared with the standard morpholino group ($P = 0.11$).

Comparison of the Volume of Neovascularization and Inflammatory Infiltration

The Flt morpholino group ($n = 18$) showed significantly less neovascularization volume ($0.737 \times 10^7 \pm 0.100 \times 10^7$ μm^3) when compared with the standard morpholino ($2.627 \times 10^7 \pm 0.250 \times 10^7$, $P = 0.000$, $n = 28$) and the PBS groups ($2.339 \times 10^7 \pm 0.391 \times 10^7$, $P = 0.001$, $n = 24$) (Fig. 5). The Flt morpholino group showed a trend toward reduced macrophage and monocyte infiltration ($0.211 \times 10^7 \pm 0.024 \times 10^7$) when compared with the STD morpholino group ($0.346 \times 10^7 \pm 0.057 \times 10^7$), but this reduction did not reach statistical significance ($P = 0.07$). There was no difference in inflammatory cell infiltration between the Flt morpholino and PBS groups ($0.223 \times 10^7 \pm 0.024 \times 10^7$, $P = 0.72$).

Discussion

Corneal angiogenesis is driven by VEGF-A,[6,7,22] a major regulator of angiogenesis in the VEGF family.[7,8] VEGFR1 and VEGFR2 are expressed primarily on endothelial cells where they predominantly play a role in the regulation of blood vessel angiogenesis, blood vessel maintenance, endothelial cell migration, endothelial cell proliferation, blood vessel permeability,

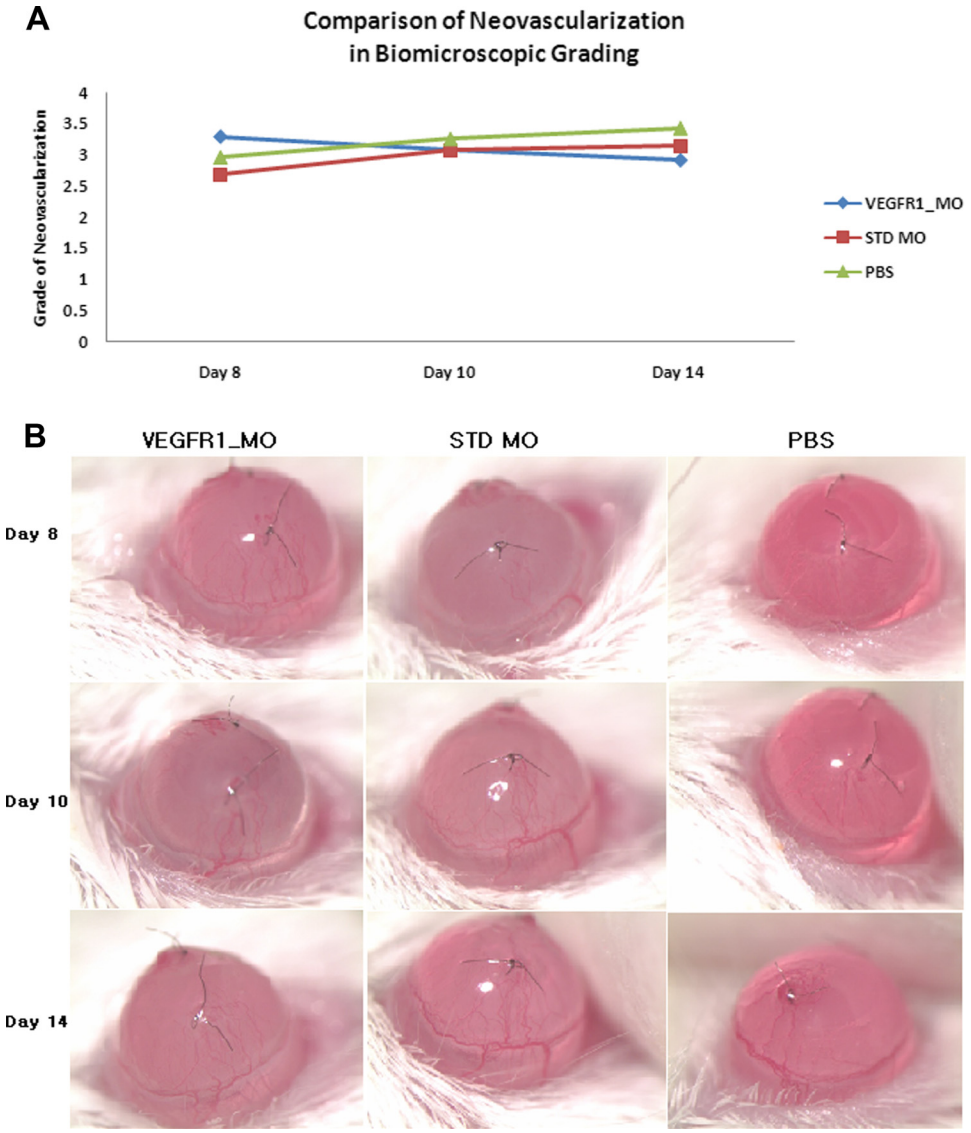

Figure 3. Comparison of in vivo neovascularization by grading. (**A**) Comparison of the grade of neovascularization in each of the three groups on days 8, 10, and 14 after suture placement. Regression of neovascularization was seen in the Flt morpholino group ($P = 0.026$), whereas the standard morpholino ($P = 0.001$) and PBS ($P = 0.005$) groups had an increase in neovascularization. A total of 24 suture sites were graded in the FLT morpholino group, 28 suture sites in the standard morpholino group, and 24 suture sites in the PBS group. (**B**) Representative images of the murine cornea model treated with Flt morpholino, standard morpholino, and PBS.

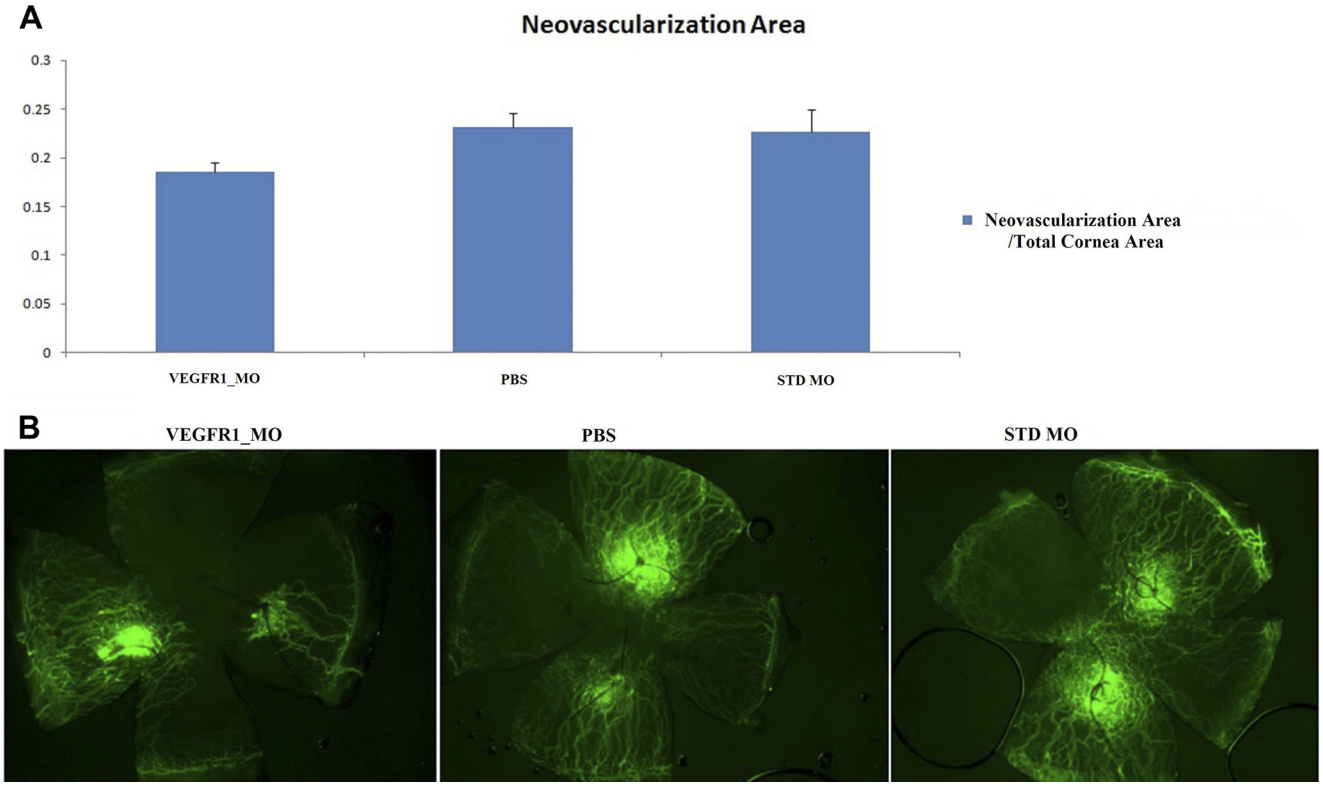

FIGURE 4. Comparison of neovascularization area. (**A**) Comparison of the neovascularized area of each treatment group. The Flt morpholino group showed a reduced area of neovascularization compared with the PBS group ($P = 0.019$). Twelve corneas in the Flt morphoino group, 14 corneas in the standard morpholino group, and 12 corneas in the PBS group were compared. (**B**) Representative pictures of corneal neovascularization in each group using fluorescent microscopy.

and dilation of blood vessels.[7,8,12] VEGFR1 is expressed not only by vascular endothelial cells but also by monocytes and macrophages[10,11] and plays a major role in migration, activation, cell survival, and expression of several proangiogenic factors for these cell types.[9,10] Monocytes and macrophages express a significant amount of VEGFR1 mRNA, but very little VEGFR2 mRNA.[9]

Because sFlt-1 is believed to play a role in the sequestration of VEGF, strategies to increase the levels of sFlt-1 may lead to reduced angiogenesis.[8,9,23] In this study, we hypothesized that morpholinos can target the alternative splicing of Flt-1 pre-mRNA to upregulate the production of sFlt-1, thereby limiting neovascularization. We observed an increase in sFlt-1 levels in the Flt morpholino groups compared with the control groups. This was associated with reduced angiogenesis. Furthermore, the Western blot results provide evidence for the disruption of mFlt-1 production in corneas treated with the Flt morpholino. When we used the antibody specific for the C terminus of VEGFR1, we found an 80-kDa band that was not present in the normal cornea group but was increased in the STD morpholino and PBS groups and decreased in the Flt morpholino group. Although the full size of mFlt-1 is approximately 180 kDa,[9,23,24] a 60- to 80-kDa band of the cytosolic portion of mFlt-1 can be found by proteolytic cleavage of mFlt-1.[8,13,25] As a result, we conclude that this 80-kDa band was the cytosolic portion of mFlt-1 produced by proteolytic cleavage of the full-length mFlt-1. Potential mechanisms for the generation of sFLT-1 include alternative mRNA splicing or proteolytic cleavage of the ectodomain. Rahimi et al.[26] showed that the cytoplasmic fragment is generated by proteolytic cleavage of the full-length VEGFR1 and Cai et al.[25] found the intracellular domain of VEGFR1 was generated by proteolysis of VEGFR1. We believe that increased levels of mFlt-1 seen in the PBS group were primarily due to the inflammation and injury caused by suture placement and were not related to the injection of PBS.

The increase of the sFlt-1/mFlt-1 ratio at the mRNA level seen with the VEGFR1 morpholino compared with the STD morpholino suggests that the VEGFR1 morpholino specificity can influence the balance of Flt-1 in corneal tissue by upregulating sFlt-1 and downregulating mFlt-1. Although there was a significant difference between the two morpholino treatment groups, we did not find a difference between the VEGFR1 morpholino and PBS treatment groups using RT-PCR. One reason for this may be related to apoptosis near the suture location induced by the VEGFR1 morpholino. After apoptosis occurs, RNA may be unstable when exposed to the extracellular environment and easily degraded. However, the partial protein is more stable and remains in extracellular matrix long enough to be detected by Western blot.

Morpholinos are just one of the available gene knockdown agents.[14,16–18] Compared with other gene knockdown agents, including phosphorothioate-linked DNA (S-DNA) and short interfering RNA (siRNA), morpholinos are not dependent on RNase H and do not have significant interaction with extracellular and cellular structures, which can result in off-target effects. In addition, morpholinos have an exceptionally high targeting success rate (70–98% knockdown of the expression of their intended target), which is likely a consequence of their high affinity for complementary RNA sequences.[16–18]

For the regression component of this study, sutures were used to induce corneal inflammation and neovascularization before treatment. Ideally, the levels of neovascularization would be similar for all groups immediately before the treatment injection. In practice, there is intrinsic phenotypic variability despite protocol standardization with single surgeon, technique, and identical instruments. In this study, the Flt

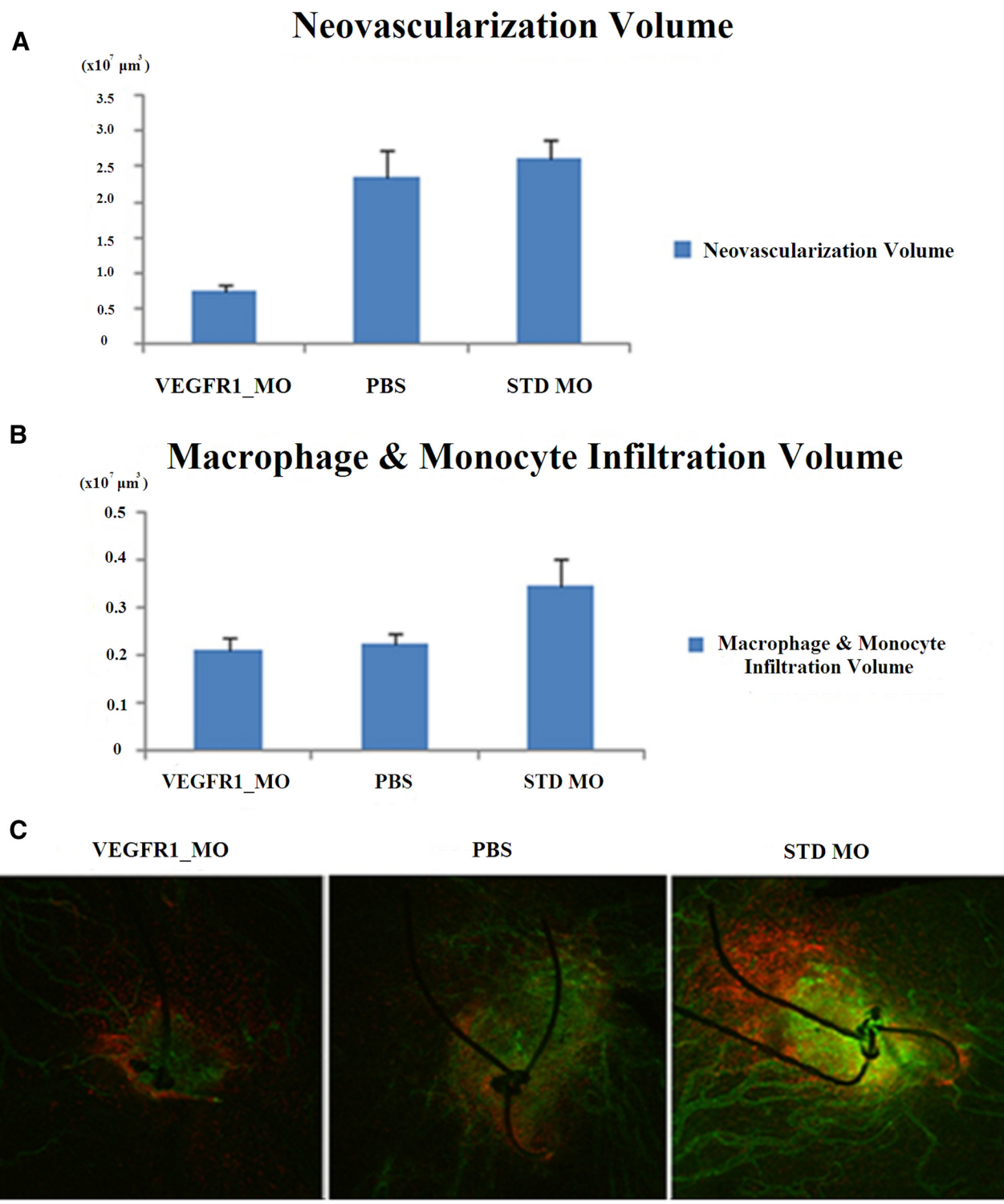

Figure 5. Comparison of volume of neovascularization and inflammatory infiltration. (**A**) Neovascularization volume measured by confocal imaging using CD31 staining. The Flt morpholino treatment group showed less neovascularization compared with the STD morpholino ($P < 0.01$) and PBS treatment groups ($P < 0.01$). (**B**) Macrophage and monocyte infiltration volume did not differ between treatment groups (as measured by confocal imaging using CD11b staining). Analysis included 18 suture sites in the Flt morpholino group, 24 suture sites in the PBS group, and 28 suture sites in the STD morpholino group. (**C**) Representative pictures of the two-dimensional horizontal planes used to measure macrophage and monocyte infiltration (*green*, CD31 staining; *red*, CD11b staining).

morpholino group showed a higher grade of neovascularization compared with that of the other groups before the treatment injection ($P < 0.031$). This difference was likely a result of inherent variation in the animal models used and inherent limitations in replicating the degree of injury in each cornea; however, this indicates a greater challenge for Flt morpholino efficacy. Although the Flt morpholino group started with a higher level of neovascularization, by day 14 this group had a lower level of neovascularization compared with that of the other treatment groups. It was also noted that in some of the

models, one side of the cornea appeared to be more affected by the treatment injection. Because we initially believed the 4 μL injection was sufficient to spread throughout the intrastomal layer, we made only one treatment injection per cornea. Although the treatments had an effect at both suture sites, the increased concentration near the site of injection may have caused the variation in treatment effect seen within the same cornea.

In our experiments we used vivo-morpholinos that are coupled to eight guanidinium head groups on dendrimer scaffolds to enable delivery into stromal cells. The molecular weight of the morpholino is approximately 8 to 9 kDa. At physiologic pH, the guanidine groups on the morpholinos are positively charged.[19,20,27–29] Because the glycosaminoglycan groups of the corneal stroma are anionic, the morpholino is unlikely to diffuse across the endothelium. Our observation of anti-angiogenic effects (e.g., less angiogenesis near the injection site) suggests limited diffusion with the distribution of the oligo-dendrimer complex remaining concentrated near the zone of injection. In the mouse cornea, the injected volume results in an injection zone that covers almost the whole cornea.

Although our results show a decrease in neovascularization with Flt morpholino treatment, we did not find a significant decrease in monocyte or macrophage levels between any of the groups. Although the comparison between the Flt morpholino group and standard morpholino group did not show a statistically significant difference ($P = 0.07$), we would expect a larger sample size to reach statistical significance. One possible explanation for the lack of a difference is that the duration from the suture placement to the treatment injection was too long. Macrophage migration to the wound site occurs 1 to 3 days after injury and with peak activation approximately 5 to 6 days after angiogenic stimuli.[30–33] Because our injection occurred outside of this time frame, it may have been too late in the inflammatory process to inhibit the VEGF and other signaling processes. A second possible explanation is that, although VEGFR1 exists on both endothelial cells and macrophages,[10,11] morpholinos may preferentially inhibit membrane-bound Flt-1 in endothelial cells. Thus, although the VEGF–VEGFR signaling for endothelial cells was disrupted, the effects on macrophage and monocyte signaling were not strong enough to reduce their volume.

Finally, in two suture sites of the corneas treated with the Flt morpholino, on day 10 we noted slightly more engorged vessels compared with day 8. One possible explanation that has been proposed is that this may have been due to a non-specific temporary toxicity in the area of the corneal injection of the morpholino.[14] Thus, further research is required to determine the optimal therapeutic concentration of morpholino treatment to minimize this potential toxicity while taking advantage of the benefits of decreased angiogenesis.

In conclusion, a morpholino targeting the exon 13/intron 13 junction of the Flt-1 transcript reduced expression of mFlt-1 and increased expression of sFlt-1, which resulted in decreased corneal angiogenesis in our murine corneal suture model.

Acknowledgments

The authors thank Jackie Simonis and Thomas Olsen for their assistance with this study.

References

1. Maddula S, Davis DK, Maddula S, Burrow MK, Ambati BK. Horizons in therapy for corneal angiogenesis. *Ophthalmology.* 2011;118:591–599.
2. Rocher N, Behar-Cohen F, Pournaras JA, et al. Effects of rat anti-VEGF antibody in a rat model of corneal graft rejection by topical and subconjunctival routes. *Mol Vis.* 2011;17:104–112.
3. Cursiefen C, Chen L, Borges LP, et al. VEGF-A stimulates lymphangiogenesis and hemangiogenesis in inflammatory neovascularization via macrophage recruitment. *J Clin Invest.* 2004;113:1040–1050.
4. Santos LN, de Moura LR, Fernandes BF, Cheema DP, Burnier MN Jr. Histopathological study of delayed regraft after corneal graft failure. *Cornea.* 2011;30:167–170.
5. Weisbrod DJ, Sit M, Naor J, Slomovic AR. Outcomes of repeat penetrating keratoplasty and risk factors for graft failure. *Cornea.* 2003;22:429–434.
6. Olsson AK, Dimberg A, Kreuger J, Claesson-Welsh L. VEGF receptor signaling: in control of vascular function. *Nat Rev Mol Cell Biol.* 2006;7:359–371.
7. Ferrara N, Kerbel RS. Angiogenesis as a therapeutic target. *Nature.* 2005;438:967–974.
8. Wu FTH, Stefanini MO, Mac Gabhann F, Kontos CD, Annex BH, Popel AS. A systems biology perspective on sVEGFR1: its biological function, pathogenic role and therapeutic use. *J Cell Mol Med.* 2010;14(3):528–552; doi:10.1111/j.1582–4934.2009.00941.x.
9. Shibuya M. Structure and dual function of vascular endothelial growth factor receptor-1 (Flt-1). *Int J Biochem Cell Biol.* 2001;33:409–420.
10. Shibuya M. Differential roles of vascular endothelial growth factor receptor-1 and receptor-2 in angiogenesis. *J Biochem Mol Biol.* 2006;39:469–478.
11. Kerber M, Reiss Y, Wickersheim A, et al. Flt-1 signaling in macrophages promotes glioma growth in vivo. *Cancer Res.* 2008;68:7342–7351.
12. Huckle WR, Roche RI. Post-transcriptional control of expression of sFlt-1, an endogenous inhibitor of vascular endothelial growth factor. *J Cell Biochem.* 2004;93:120–132.
13. Rahimi N, Golde TE, Meyer RD. Identification of ligand-induced proteolytic cleavage and ectodomain shedding of VEGFR-1/FLT1 in leukemic cancer cells. *Cancer Res.* 2009;69:2607–2614.
14. Heasman J. Morpholino oligos: making sense of antisense? *Dev Biol.* 2002;243:209–214.
15. Ekker SC, Larson JD. Morphant technology in model developmental systems. *Genesis.* 2001;30:89–93.
16. Summerton J, Weller D. Morpholino antisense oligomers: design, preparation, and properties. *Antisense Nucleic Acid Drug Dev.* 1997;7:187–195.
17. Summerton J. Morpholino antisense oligomers: the case for an RNase H-independent structural type. *Biochim Biophys Acta.* 1999;1489:141–158.
18. Summerton JE. Morpholino, siRNA, and S-DNA compared: impact of structure and mechanism of action on off-target effects and sequence specificity. *Curr Top Med Chem.* 2007;7:651–660.
19. Morcos PA, Li Y, Jiang S. Vivo-morpholinos: a non-peptide transporter delivers morpholinos into a wide array of mouse tissues. *BioTechniques.* 2008;45:613–623.
20. Moulton JD, Jiang S. Gene knockdowns in adult animals: PPMOs and vivo-morpholinos. *Molecules.* 2009;14:1304–1323.
21. Singh N, Amin S, Richter E, et al. Flt-1 intraceptors inhibit hypoxia-induced VEGF expression in vitro and corneal neovascularization in vivo. *Invest Ophthalmol Vis Sci.* 2005;46:1647–1652.
22. Ferrara N. Vascular endothelial growth factor: basic science and clinical progress. *Endocr Rev.* 2004;25:581–611.
23. Ambati BK, Nozaki M, Singh N, et al. Corneal avascularity is due to soluble VEGF receptor-1. *Nature.* 2006;443:993–997.
24. Mittar S, Ulyatt C, Howell GJ, et al. VEGFR1 receptor tyrosine kinase localization to the Golgi apparatus is calcium-dependent. *Exp Cell Res.* 2009;315:877–889.
25. Cai J, Jiang WG, Grant MB, Boulton M. Pigment epithelium-derived factor inhibits angiogenesis via regulated intracellular proteolysis of vascular endothelial growth factor receptor 1. *J Biol Chem.* 2006;281:3604–3613.
26. Rahimi N, Golde TE, Meyer RD. Identification of ligand-induced proteolytic cleavage and ectodomain shedding of VEGFR-1/FLT1 in leukemic cancer cells. *Cancer Res.* 2009;69:2607–2614.
27. Wu B, Li Y, Morcos PA, Doran TJ, Lu P, Lu QL. Octa-guanidine morpholino restores dystrophin expression in cardiac and skeletal

muscles and ameliorates pathology in dystrophic mdx mice. *Mol Ther.* 2009;17:864–871.

28. Hodson S, Kaila D, Hammond S, Rebello G, al-Omari Y. Transient chloride binding as a contributing factor to corneal stromal swelling in the ox. *J Physiol.* 1992;450:89–103.
29. Bonduelle CV, Gillies ER. Dendritic guanidines as efficient analogues of cell penetrating peptides. *Pharmaceuticals.* 2010;3:636–666; doi:10.3390/ph3030636.
30. Maruyama K, Ii M, Cursiefen C, et al. Inflammation-induced lymphangiogenesis in the cornea arises from CD11b-positive macrophages. *J Clin Invest.* 2005;115:2363–2372.
31. Nakao S, Kuwano T, Tsutsumi-Miyahara C, et al. Infiltration of COX-2-expressing macrophages is a prerequisite for IL-1 beta-induced neovascularization and tumor growth. *J Clin Invest.* 2005;115:2979–2991.
32. Frank S, Hubner G, Breier G, Longaker MT, Greenhalgh DG, Werner S. Regulation of vascular endothelial growth factor expression in cultured keratinocytes. Implications for normal and impaired wound healing. *J Biol Chem.* 1995;270:12607–12613.
33. Hos D, Saban DR, Bock F, et al. Suppression of inflammatory corneal lymphangiogenesis by application of topical corticosteroids. *Arch Ophthalmol.* 2011;129:445–452.